# **Tube-Certified Trajectory Tracking for Nonlinear Systems With Robust Control Contraction Metrics**

Pan Zhao<sup>1</sup>, Arun Lakshmanan<sup>1</sup>, Kasey Ackerman<sup>1</sup>, Aditya Gahlawat<sup>1</sup>, Marco Pavone<sup>2</sup>, and Naira Hovakimyan<sup>1</sup>

Abstract—This paper presents an approach towards guaranteed trajectory tracking for nonlinear control-affine systems subject to external disturbances based on robust control contraction metrics (CCM) that aims to minimize the  $\mathcal{L}_{\infty}$  gain from the disturbances to nominal-actual trajectory deviations. The guarantee is in the form of invariant tubes, computed offline and valid for any nominal trajectories, in which the actual states and inputs of the system are guaranteed to stay despite disturbances. Under mild assumptions, we prove that the proposed robust CCM (RCCM) approach yields tighter tubes than an existing approach based on CCM and input-to-state stability analysis. We show how the RCCM-based tracking controller together with tubes can be incorporated into a feedback motion planning framework to plan safe trajectories for robotic systems. Simulation results illustrate the effectiveness of the proposed method and empirically demonstrate reduced conservatism compared to the CCM-based approach.

Index Terms—Planning under uncertainty, robot safety, integrated planning and control, robust control, nonlinear systems

#### I. INTRODUCTION

Motion planning for robots with nonlinear and underactuated dynamics – with guaranteed safety in the presence of uncertainties – remains to be a challenging problem. The uncertainties can cause the robot's actual state trajectory to significantly deviate from its nominal behavior, causing collisions, especially when a nominal input trajectory is executed in an open-loop fashion (see Fig. 1). Feedback motion planning (FMP) aims to mitigate the effect of uncertainties through the use of a feedback controller that tracks a nominal (or desired) trajectory. A common practice in FMP to ensure vehicle safety with respect to dynamic constraints and collision avoidance involves design of the tracking controller and computation of a tube or funnel around the nominal trajectory which is guaranteed to contain the actual trajectory despite uncertainties.

**Related Work**: Various methods have been proposed for computing and/or optimizing such tubes or funnels in nonlinear setting. For the special case of fully-actuated systems, the tubes or funnels may be computed and optimized using sliding

Manuscript received: September 9, 2021; Revised December 26, 2021; Accepted February 1, 2022. This paper was recommended for publication by Editor Clement Gosselin upon evaluation of the Associate Editor and Reviewers' comments. This work is supported by AFOSR and NSF under the NRI grants #1830639 and #1830554, and RI grant #2133656. (Corresponding author: Pan Zhao.)

<sup>1</sup>P. Zhao, A. Lakshmanan, K. Ackerman, A. Gahlawat and N. Hovakimyan are with the Department of Mechanical Science and Engineering, University of Illinois at Urbana-Champaign, Urbana, IL 61801, USA. {panzhao2, lakshma2, gahlawat, kaacker2, nhovakim}@illinois.edu.

<sup>2</sup>M. Pavone is with the Department of Aeronautics and Astronautics, Stanford University, Stanford, CA 94305, USA. pavone@stanford.edu. Digital Object Identifier (DOI): see top of this page.

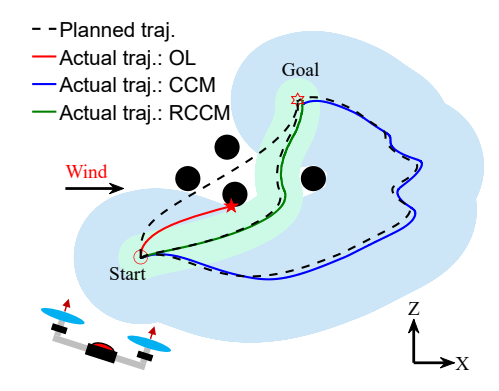


Fig. 1: Planning and control of a planar VTOL vehicle under wind disturbances. Light blue and green shaded areas denote the tubes associated with a CCM controller from [3], and the proposed RCCM controller, respectively. Dashed lines denote the trajectories planned without using tubes (left) and with CCM (right) and RCCM (middle) tubes. OL: open loop.

mode control [1]. In [2], the authors used linear analysis (i.e., propagation of ellipsoids under linearized dynamics) to compute the size of approximate invariant funnels, and further leveraged it to optimize the nominal trajectory. However, the linearity assumption only holds in a small region around the particular nominal trajectory. Convex programming-based verification methods such as sum of squares (SOS) programming have also gained popularity in FMP. For instance, the LQR tree algorithms in [4], [5] combines local LQR feedback controllers with funnels to compose a nonlinear feedback policy to cover reachable areas. However, users are restricted to a *fixed set* of trajectories computed offline when applying these algorithms.

The concept of tubes has been explored extensively within Tube Model Predictive Control (TMPC), where one computes a tracking feedback (also termed as ancillary) controller that keeps the state within an invariant tube around the nominal MPC trajectory despite disturbances. For instance, assuming the existence of a stabilizing feedback controller and a Lyapunov function, [6] constructed a tube based on a Lipschitz constant of the dynamics. This approach, however, becomes very conservative for larger prediction horizons. For the special case of feedback linearizable systems, [7] used a boundary layer sliding controller as an auxiliary controller, which enables the tube to be parameterized as a polytope and its geometry to be co-optimized in the MPC problem. Recently in [8], for incrementally stabilizable nonlinear systems subject to state and input dependent disturbances, the authors leveraged scalar bounds of an incremental Lyapunov function, computed offline, to online predict the tube size.

Recent work has explored contraction theory for FMP.

Contraction theory [9] is a method for analyzing nonlinear systems in a differential framework and is focused on studying the convergence between pairs of state trajectories towards each other, i.e., incremental stability. It has recently been extended for constructive control design via control contraction metrics (CCM) [10], [11]. Leveraging CCM, the authors of [3] designed a tracking controller for a nominal nonlinear system and derived tubes in which the actual states are guaranteed to remain despite disturbances via input-to-state stability (ISS) analysis. For systems with matched uncertainties, the authors of [12] designed an  $\mathcal{L}_1$  adaptive controller to augment a nominal CCM controller and showed that the resulting tube's size could be systematically reduced by tuning some parameters of the adaptive controller, while the method in [13] – based on robust Riemannian energy conditions and disturbance estimation – guaranteed exponential convergence to nominal trajectories despite the uncertainties. Finally, robust CCM was leveraged in [14] to synthesize nonlinear controllers that minimize the  $\mathcal{L}_2$  gain from disturbances to outputs. This method, however, does not provide tubes to quantify the transient behavior of states and inputs.

Statement of Contributions: For nonlinear control-affine systems subject to bounded disturbances, this paper presents a tracking controller based on robust CCM (RCCM) to minimize the  $\mathcal{L}_{\infty}$  gain from disturbances to nominal-actual trajectory deviations. By solving convex optimization problems offline, the proposed RCCM scheme produces a fully nonlinear tracking controller with explicit disturbance rejection property together with certificate tubes around nominal trajectories, for both states and inputs, in which the actual state/input variables are guaranteed to stay despite disturbances. We further prove, under mild assumptions, that the proposed RCCM approach yields tighter tubes than the CCM approach in [3], which ignores the disturbance in designing the tracking controller and relies on ISS analysis to derive the tubes. Additionally, we illustrate how the RCCM controller and the tubes can be incorporated into an FMP framework to plan safe trajectories, and verify the proposed scheme on a planar vertical take-off and landing (VTOL) vehicle and a 3D quadrotor. Compared to the CCM approach, our RCCM approach demonstrates improved tracking performance and reduced tube size for both states and inputs, leading to more aggressive yet safe trajectories (See Fig. 1).

Notations. Let  $\mathbb{R}^n$ ,  $\mathbb{R}^+$  and  $\mathbb{R}^{m \times n}$  denote the n-dimensional real vector space, the set of non-negative real numbers, and the set of real m by n matrices, respectively.  $I_n$  and 0 denote an  $n \times n$  identity matrix, and a zero matrix of compatible dimensions, respectively.  $\|\cdot\|$  denotes the 2-norm of a vector or a matrix. The space  $\mathcal{L}_{\infty e}$  is the set of signals on  $[0,\infty)$  which, truncated to any finite interval [a,b], have finite amplitude. The  $\mathcal{L}_{\infty}$ - and truncated  $\mathcal{L}_{\infty}$ -norm of a function  $x:\mathbb{R}^+ \to \mathbb{R}^n$  are defined as  $\|x\|_{\mathcal{L}_{\infty}} \triangleq \sup_{t \geq 0} \|x(t)\|$  and  $\|x\|_{\mathcal{L}_{\infty}^{[0,T]}} \triangleq \sup_{0 \leq t \leq T} \|x(t)\|$ , respectively. Let  $\partial_y F(x)$  denote the Lie derivative of the matrix-valued function F at x along the vector y. For symmetric matrices P and P0 and P1 along the vector P2 is positive definite (semidefinite). P3 is the shorthand notation of P3.

#### II. PROBLEM STATEMENT AND PRELIMINARIES

Consider a nonlinear control-affine system

$$\dot{x} = f(x) + B(x)u + B_w(x)w, \quad z = g(x, u),$$
 (1)

where  $x(t) \in \mathbb{R}^n$  is the state vector,  $u(t) \in \mathbb{R}^m$  is the control input vector,  $w(t) \in \mathbb{R}^p$  is the disturbance vector and  $z(t) \in \mathbb{R}^q$  denotes the variables related to the performance (with z = x or z = u as a special case), and f(x), B(x) and  $B_w(x)$  are known vector/matrix functions of compatible dimensions. We use  $b_i$  and  $b_{w,i}$  to represent the ith column of B(x) and  $B_w(x)$ , respectively.

For system (1), assume we have a nominal state and input trajectory,  $x^*(\cdot)$  and  $u^*(\cdot)$ , satisfying the nominal dynamics:

$$\dot{x}^* = f(x^*) + B(x^*)u^* + B_w(x^*)w^*, \quad z^* = g(x^*, u^*), \quad (2)$$

where  $w^*$  is the vector of nominal disturbances (including  $w^*(t) \equiv 0$  as a special case). This paper is focused on designing a state-feedback controller in the form of

$$u(t) = k(x(t), x^*(t)) + u^*(t)$$
 (3)

to minimize the gain from disturbance deviation,  $w-w^*$ , to output deviation,  $z-z^*$ , of the closed-loop system (obtained by applying the controller (3) to (1)):

$$\dot{x} = f(x) + B(x) (k(x, x^*) + u^*) + B_w(x)w, z = q(x, k(x, x^*) + u^*)$$
(4)

Formally, such gain is quantified using the concept of *universal*  $\mathcal{L}_{\infty}$  gain defined as follows. Hereafter, we use universal  $\mathcal{L}_{\infty}$  gain and  $\mathcal{L}_{\infty}$  gain interchangeably.

**Definition 1.** (Universal  $\mathcal{L}_{\infty}$  gain) A control system (4) achieves a universal  $\mathcal{L}_{\infty}$ -gain bound of  $\alpha$  if for any target trajectory  $x^{\star}, w^{\star}, z^{\star}$  satisfying (4), any initial condition x(0), and input w such that  $w - w^{\star} \in \mathcal{L}_{\infty e}$ , the condition

$$||z-z^{\star}||_{\mathcal{L}_{\infty}^{[0,T]}}^{2} \leq \alpha^{2} ||w-w^{\star}||_{\mathcal{L}_{\infty}^{[0,T]}}^{2} + \beta(x(0), x^{\star}(0)), \ \forall T > 0,$$
(5)

holds for a function  $\beta(x_1, x_2) \ge 0$  with  $\beta(x, x) = 0$  for all x.

Remark 1. The  $\mathcal{L}_{\infty}$ -gain bound  $\alpha$  in Definition 1 naturally gives certificate tubes to quantify how much the actual trajectory  $z(\cdot)$  deviates from the nominal trajectory  $z^*(\cdot)$ . For instance, by setting z=x and  $x(0)=x^*(0)$  and using a worst-case estimate of  $\|w-w^*\|_{\mathcal{L}^{[0,T]}_{\infty}}$ , denoted by  $\bar{w}$  (i.e.,  $\|w-w^*\|_{\mathcal{L}^{[0,T]}_{\infty}}\leq \bar{w}$ ), the inequality (5) implies  $x\in\Omega(x^*)\triangleq \left\{y\in\mathbb{R}^n:\|y-x^*\|_{\mathcal{L}^{[0,T]}_{\infty}}\leq \alpha \bar{w}\right\}$  for any T>0.

Remark 2. Definition 1 is inspired by the concept of universal  $\mathcal{L}_2$  gain in [14]. However, unlike the  $\mathcal{L}_{\infty}$  gain in Definition 1, the  $\mathcal{L}_2$  gain does not produce tubes to quantify the *transient* behavior of the variable z.

#### A. Preliminaries

CCM is a tool for controller synthesis to ensure incremental stability of a nonlinear system by studying the variational system, characterized by the differential dynamics [10]. In this paper, we propose RCCM to design the controller (3)

to achieve or minimize an  $\mathcal{L}_{\infty}$ -gain bound. The differential dynamics associated with (1) are given by

$$\dot{\delta}_x = A(x, u, w)\delta_x + B(x)\delta_u + B_w(x)\delta_w,$$

$$\delta_z = C(x, u)\delta_x + D(x, u)\delta_u.$$
(6)

where  $A(x,u,w) \triangleq \frac{\partial f}{\partial x} + \sum_{i=1}^{m} \frac{\partial b_{i}}{\partial x} u_{i} + \sum_{i=1}^{p} \frac{\partial b_{w,i}}{\partial x} w_{i}, C(x,u) \triangleq$ 

 $\begin{array}{l} \frac{\partial g}{\partial x} \text{ and } D(x,u) \triangleq \frac{\partial g}{\partial u}. \\ \text{Defining } K(x,x^{\star}) \triangleq \frac{\partial k}{\partial x} \text{ with } k \text{ characterizing the control law (3), we obtain the differential dynamics of the closed-loop} \end{array}$ system (4) as

$$\dot{\delta}_x = \mathcal{A}\delta_x + \mathcal{B}\delta_w, \quad \delta_z = \mathcal{C}\delta_x + \mathcal{D}\delta w, \tag{7}$$

where

$$\mathcal{A} \triangleq (A + BK), \ \mathcal{B} = B_w, \ \mathcal{C} \triangleq (C + DK), \ \mathcal{D} = 0.$$
 (8)

Our solution also involves the differential  $\mathcal{L}_{\infty}$  gain, defined as follows.

**Definition 2.** (Differential  $\mathcal{L}_{\infty}$  gain) A system with its differential dynamics represented by (7) has a differential  $\mathcal{L}_{\infty}$ -gain bound of  $\alpha > 0$ , if for all T > 0 one has

$$\|\delta_z\|_{\mathcal{L}_{\infty}^{[0,T]}}^2 \le \alpha^2 \|\delta_w\|_{\mathcal{L}_{\infty}^{[0,T]}}^2 + \beta(x(0), \delta_x(0)), \tag{9}$$

for some function  $\beta(x, \delta x)$  with  $\beta(x, 0) = 0$  for all x.

Before moving to the next section, we now introduce some notations related to Riemannian geometry. A Riemannian metric on  $\mathbb{R}^n$  is a symmetric positive-definite matrix function M(x), smooth in x, which defines a "local Euclidean" structure for any two tangent vectors  $\delta_1$  and  $\delta_2$  through the inner product  $\langle \delta_1, \delta_2 \rangle_x \triangleq \delta_1^\top M(x) \delta_2$  and the norm  $\sqrt{\langle \delta_1, \delta_2 \rangle_x}$ . A metric is called uniformly bounded if  $a_1I \leq M(x) \leq a_2I$ holds  $\forall x$  and for some scalars  $a_2 \geq a_1 > 0$ . Let  $\Gamma(a, b)$  be the set of smooth paths between two points a and b in  $\mathbb{R}^n$ , where each  $c \in \Gamma(a,b)$  is a piecewise smooth mapping,  $c:[0,1] \to$  $\mathbb{R}^n$ , satisfying c(0) = a, c(1) = b. We use the notation  $c(s), s \in [0,1], \text{ and } c_s(s) \triangleq \frac{\partial c}{\partial s}.$  Given a metric M(x), the energy of a path c is defined as  $E(c) \triangleq \int_0^1 c_s^\top M(c(s)) c_s(s) ds$ . We also use the notation E(a, b) to denote the minimal energy of a path joining a and b, i.e.,  $E(a, b) \triangleq \inf_{c \in \Gamma(a, b)} E(c)$ .

## III. ROBUST CCM FOR TUBE-CERTIFIED TRAJECTORY **TRACKING**

We first introduce an approach to designing a fully nonlinear controller in the form of (3) to achieve a given  $\mathcal{L}_{\infty}$ -gain bound or minimize such a bound, leveraging RCCM. We then present the derivation and optimization of the certificate tubes around nominal state and control input trajectories, in which the actual states and inputs are guaranteed to stay.

# A. RCCM for universal $\mathcal{L}_{\infty}$ gain guarantee

Existing work, e.g., [15], provides solutions to controller design for a linear time-invariant (LTI) system for standard  $\mathcal{L}_{\infty}$ -gain guarantee/minimization using linear matrix inequality (LMI) techniques. We now extend this result to nonlinear systems for differential  $\mathcal{L}_{\infty}$ -gain guarantee/minimization, summarized in the following lemma. The proof is similar to the LTI case and is included in [16] due to space limit.

**Lemma 1.** The closed-loop system (4) has a differential  $\mathcal{L}_{\infty}$ gain bound of  $\alpha > 0$  if there exists a uniformly-bounded symmetric metric M(x) > 0 and positive constants  $\lambda$  and  $\mu$  such that for all x, w, we have

$$\begin{bmatrix} \langle M\mathcal{A} \rangle + \dot{M} + \lambda M & M\mathcal{B} \\ \mathcal{B}^{\top} M & -\mu I_p \end{bmatrix} \le 0, \tag{10}$$

3

$$\begin{bmatrix} \langle M\mathcal{A} \rangle + \dot{M} + \lambda M & M\mathcal{B} \\ \mathcal{B}^{\top}M & -\mu I_{p} \end{bmatrix} \leq 0, \tag{10}$$

$$\begin{bmatrix} \lambda M & 0 & \mathcal{C}^{\top} \\ 0 & (\alpha - \mu)I_{p} & \mathcal{D}^{\top} \\ \mathcal{C} & \mathcal{D} & \alpha I_{q} \end{bmatrix} \geq 0, \tag{11}$$

where  $\dot{M} \triangleq \sum_{i=1}^{n} \frac{\partial M}{\partial x_{i}} \dot{x}_{i}$  with  $\dot{x}_{i}$  given by (4).

Remark 3. In case the metric M(x) depends on  $x_i$ , an element of x, whose derivative is dependent on the input u (or w), Mand thus the condition (10) will depend on u (or w). In this case, a bound on u (or w) needs to be known in order to verify the conditions (10) and (11).

We term the metric  $V(x, \delta_x) = \delta_x^{\top} M(x) \delta_x$  as a robust CCM (RCCM). Given a closed-loop system, Lemma 1 provides conditions to check whether a constant is a differential  $\mathcal{L}_{\infty}$ gain bound of the system. We next address the problem of how to design a controller to achieve a desired universal  $\mathcal{L}_{\infty}$ -gain bound given an open-loop plant (1).

Control law construction: Similar to [14], we use M(x) as a Riemannian metric to choose the path of minimum energy joining x and  $x^*$  and construct the control law:

$$\gamma(t) = \arg_{c \in \Gamma(x(t), x^{\star}(t))} \min E(c)$$
 (12a)

$$u(t) = u^{\star}(t) + \int_{0}^{s} K(\gamma(t,s)) \frac{\partial \gamma(t,s)}{\partial s} ds,$$
 (12b)

where  $E(c) \triangleq \int_0^1 c_s^{\top} M(c(s)) c_s(s) ds$  and the matrix function  $K(\cdot)$  will be introduced later in (13) and (14). Following [10], we make the following assumption to simplify the subsequent analysis.

**Assumption 1.** For the control system (1), (12), the set of times  $t \in [0, \infty)$  for which x(t) is in the cut locus of  $x^*(t)$ has zero measure.

Without this assumption, the main results (Theorem 1) still hold if the derivative of the Riemannian energy,  $E(x, x^*)$ , used in proof of Theorem 1, is replaced with its upper Dini derivative, as done in [3]. The main theoretical results for synthesizing a controller using RCCM to guarantee a universal  $\mathcal{L}_{\infty}$ -gain bound can now be presented.

**Theorem 1.** For the plant (1) with differential dynamics (6), suppose there exists a uniformly-bounded metric W(x) > 0, a matrix function Y(x), and positive constants  $\lambda$ ,  $\mu$  and  $\alpha$ such that

$$\begin{bmatrix} \langle AW + BY \rangle - \dot{W} + \lambda W & B_w \\ B_w^\top & -\mu I_p \end{bmatrix} \le 0, \quad (13)$$

$$\begin{bmatrix} \langle AW + BY \rangle - \dot{W} + \lambda W & B_w \\ B_w^{\top} & -\mu I_p \end{bmatrix} \leq 0, \quad (13)$$

$$\begin{bmatrix} \lambda W & \star & \star \\ 0 & (\alpha - \mu)I_p & \star \\ CW + DY & 0 & \alpha I_q \end{bmatrix} \geq 0, \quad (14)$$

for all x, u, w, where  $\dot{W} \triangleq \sum_{i=1}^{n} \frac{\partial W}{\partial x_i} \dot{x}_i$ . Then for any target trajectory  $u^*, x^*, w^*$  satisfying (2), if Assumption 1 holds, the RCCM controller (12) with

$$K(x) = Y(x)W^{-1}(x),$$
 (15)

achieves a universal  $\mathcal{L}_{\infty}$ -gain bound of  $\alpha$  for the closed-loop system.

Remark 4. From the proof of Theorem 1, one can see that W(x) in (13) and (14) is connected with M(x) in (10) and (11) by  $M(x) = W^{-1}(x)$ . This is similar to the LTI case where a matrix equal to the inverse of a Lyapunov matrix is introduced for state-feedback control design [15]. We term W(x) as a dual RCCM.

Removal of synthesis conditions' dependence on u: Condition (13) may depend on u and w due to the presence of terms A and  $\dot{W}$ . Dependence on w is not a significant issue as a bound on w can usually be pre-established and incorporated in solving the optimization problem involving (13). Since a bound on u is not easy to obtain (before a controller is synthesized), the dependence of (13) on u is undesired. To remove such dependence, we need the following condition:

(C1) For each 
$$i=1,\ldots,m,\ \partial_{b_i}W-\left\langle\frac{\partial b_i}{\partial x}W\right\rangle=0.$$
 Formally, condition (C1) states that  $b_i$  is a Killing vector for the metric  $W$  [10, Section III.A]. In particular, if  $B$  is in the form of  $[0,I_{m_1}]^{\top}$ , condition (C1) requires that  $W$  must not depend on the last  $m_1$  state variables.

# B. Offline search of RCCM for $\mathcal{L}_{\infty}$ gain minimization

The constant  $\alpha$ , which is an upper bound on the universal  $\mathcal{L}_{\infty}$  gain, appears linearly in the condition (14) of Theorem 1. Therefore, one can minimize  $\alpha$  when searching for W(x) and Y(x). To make the optimization problem feasible, one often needs to limit the states to a compact set, i.e., considering  $x \in \mathcal{X}$ , where  $\mathcal{X}$  is a compact set. Additionally, since calculating the inverse of W(x) is needed for constructing the control law due to  $M(x) = W^{-1}(x)$  (detailed in [16, Section III.D]), one may also want to enforce a lower bound,  $\underline{\beta}$ , on the eigenvalues of W(x). Therefore, in practice, one could solve the optimization problem  $\mathcal{OPT}_{RCCM}$ :

$$\mathcal{OPT}_{RCCM}: \min_{W,Y,\lambda>0,\mu>0} \alpha$$
 (16a)

$$W(x) \ge \underline{\beta} I_n,$$
 (16c)

$$x \in \mathcal{X}$$
. (16d)

#### C. Offline optimization for refining state and input tubes

In formulating the optimization problem  $\mathcal{OPT}_{RCCM}$  to search for W(x) and Y(x), the z vector often contains weighted states and inputs to balance the tracking performance and control efforts. For instance, we could have  $z = [(Qx)^\top, (Ru)^\top]^\top$ , where Q and R are some weighting matrices. After obtaining W(x) and Y(x), one can always derive refined  $\mathcal{L}_{\infty}$ -gain bounds for some specific state and

input variables,  $\hat{z} \in \mathbb{R}^l$ , by re-deriving the C and D matrices in (6) for  $\hat{z} = \hat{g}(x, u)$ , and then solving the optimization problem  $\mathcal{OPT}_{REF}$ :

$$\mathcal{OPT}_{REF}: \min_{\lambda > 0, \mu > 0} \alpha$$
 (17a)

$$x \in \mathcal{X}$$
. (17c)

For instance, by solving  $\mathcal{OPT}_{REF}$ , we get an  $\mathcal{L}_{\infty}$ -gain bound for the deviation of some states (i.e.,  $\|x_{\mathbb{I}} - x_{\mathbb{I}}^{\star}\|_{\mathcal{L}_{\infty}}$ , where  $\mathbb{I}$  is the index set) with  $\hat{z} = x_{\mathbb{I}}$ , and an  $\mathcal{L}_{\infty}$ -gain bound for the deviation of all inputs (i.e.,  $\|u - u^{\star}\|_{\mathcal{L}_{\infty}}$ ) with  $\hat{z} = u$ . With an  $\mathcal{L}_{\infty}$ -gain bound  $\alpha$  (from solving  $\mathcal{OPT}_{REF}$ ) and a bound  $\bar{w}$  on the disturbances, i.e.,  $\|w - w^{\star}\|_{\mathcal{L}_{\infty}} \leq \bar{w}$ , the actual variable  $\hat{z}$  is guaranteed to stay in a tube around the nominal variable  $\hat{z}^{\star}$ , i.e.,

$$\hat{z} \in \Omega(\hat{z}^*) \triangleq \{ y \in \mathbb{R}^l : ||y - \hat{z}^*|| \le \alpha \bar{w} \}. \tag{18}$$

Following this idea, we can easily get the tube for all or part of the states or inputs.

Remark 5. The tubes obtained through (18) hold for any trajectory that satisfy the nominal dynamics (2), and are particularly suitable to be incorporated into *online* planning and predictive control schemes, e.g., tube MPC.

Online computation of the control law is detailed in [16], and omitted here due to space limit.

### IV. APPLICATION TO FEEDBACK MOTION PLANNING

Thanks to the certificate tubes in (18), the RCCM controller presented in Section III can be conveniently incorporated as a low-level tracking or ancillary controller into a feedback motion planning or nonlinear tube MPC framework. We demonstrate an application to the former in this section. The core idea is to compute nominal motion plans  $(x^*, u^*)$  using the nominal dynamics (2) and tightened constraints. Denote the tubes for  $x-x^*$  and  $u-u^*$  obtained through solving  $\mathcal{OPT}_{REF}$  in Section III-C as  $\tilde{\Omega}_x \triangleq \{\tilde{x} \in \mathbb{R}^n : \|\tilde{x}\| \leq \alpha_x \bar{w}\}$  and  $\tilde{\Omega}_u \triangleq \{\tilde{u} \in \mathbb{R}^m : \|\tilde{u}\| \leq \alpha_u \bar{w}\}$ , where  $\alpha_x$  and  $\alpha_u$  are the universal  $\mathcal{L}_{\infty}$ -gain bounds for the states and control inputs, respectively, and  $\bar{w}$  is a bound on the disturbances, i.e.,  $\|w-w^*\|_{\mathcal{L}_{\infty}} \leq \bar{w}$ . Then, the tightened constraints are given by

$$x^{\star}(\cdot) \in \bar{\mathcal{X}} \triangleq \mathcal{X} \ominus \tilde{\Omega}_x, \ u^{\star}(\cdot) \in \bar{\mathcal{U}} \triangleq \mathcal{U} \ominus \tilde{\Omega}_u,$$
 (19)

where  $\mathcal{U}$  is the control constraint set, and  $\ominus$  denotes the Minkowski set difference. One can simply use the tightened constraints in (19) and the nominal dynamics (2) to plan a trajectory. Then, with the proposed RCCM controller, the actual states and inputs are guaranteed to stay in  $\mathcal{X}$  and  $\mathcal{U}$ , respectively, in the presence of disturbances bounded by  $\bar{w}$ .

# V. COMPARISONS WITH AN EXISTING CCM-BASED APPROACH

In [3], the authors designed a tracking controller based on CCM without considering disturbances and then derived a tube where the actual states are guaranteed to stay in the presence

of disturbances using input-to-state stability (ISS) analysis. In comparison, our method explicitly incorporates disturbance rejection in designing the RCCM controller and produces tubes for both states and inputs together with the controller (if we include the tube refining process in Section III-C as a part of the controller design process). Under mild assumptions, we will prove that the tube yielded by our method is tighter than that from applying the idea of [3]. To be consistent with the problem setting in [3], for this section, we set  $w^* \equiv 0$ in defining the nominal (i.e., un-disturbed) system (2), which leads to the nominal dynamics:

$$\dot{x}^* = f(x^*) + B(x^*)u^*. \tag{20}$$

Unlike our approach, in [3] the search of the CCM metric is not jointly done with search of a matrix function (i.e., Y(x) in Theorem 1, used to construct a differential feedback controller). Instead, [3] uses a min-norm type control law computed using only the CCM metric. To facilitate a rigorous comparison, we slightly modify the condition for the CCM metric search to include another matrix function (analogous to Y(x) in Theorem 1). Indeed, a joint search of a CCM metric W(x) and a matrix function Y(x) is adopted in [10], which [3] builds upon. Such modification only influences the control signal determination, and does not change the essential ideas of [3]. With such modifications, the main results of [3] can be summarized as follows.

**Lemma 2.** ([3]) For the nominal system (20), assume there exists a metric  $W(x^*)$ , a matrix function  $Y(x^*)$  and a constant  $\lambda > 0$  satisfying

$$-\dot{\hat{W}} + \langle \hat{A}\hat{W} + B\hat{Y} \rangle + 2\hat{\lambda}\hat{W} \le 0, \tag{21}$$

where  $\hat{A} \triangleq \frac{\partial f}{\partial x^{\star}} + \sum_{i=1}^{m} \frac{\partial b_{i}}{\partial x} u_{i}^{\star}$ ,  $\dot{\hat{W}} = \sum_{i=1}^{n} \frac{\partial \hat{W}(x^{\star})}{\partial x_{i}^{\star}} \dot{x}_{i}^{\star}$ . Furthermore,  $\hat{W}(x^*)$  is uniformly bounded, i.e.  $\beta I_n \leq \hat{W}(x^*) \leq \bar{\beta} I_n$ with  $\bar{\beta} \geq \beta > 0$ , for all  $x^* \in \mathcal{X}$ . Then, for the perturbed system (1) under the controller (12) with  $W = \hat{W}$  and  $Y = \hat{Y}$ , if  $x(0) = x^*(0)$ , we have

$$||x - x^{\star}||_{\mathcal{L}_{\infty}^{[0,T]}}^{2} \le \hat{\alpha}^{2} ||w||_{\mathcal{L}_{\infty}^{[0,T]}},$$
 (22)

where

$$\hat{\alpha} \triangleq \frac{1}{\hat{\lambda}} \sqrt{\bar{\beta}/\underline{\beta}} \sup_{x \in \mathcal{X}} \bar{\sigma}(B_w(x)), \tag{23}$$

with  $\bar{\sigma}(\cdot)$  denoting the largest singular value.

We also need the following assumption.

**Assumption 2.** The metric  $\hat{W}$  in (21) satisfies both of the following conditions:

(C2) For each 
$$i = 1, ..., m$$
,  $\partial_{b_i} \hat{W} - \left\langle \frac{\partial b_i}{\partial x} \hat{W} \right\rangle = 0$ .

(C2) For each 
$$i=1,\ldots,m,\ \partial_{b_i}\hat{W}-\left\langle\frac{\partial b_i}{\partial x}\hat{W}\right\rangle=0.$$
 (C3) For each  $i=1,\ldots,p,\ \partial_{b_{w,i}}\hat{W}-\left\langle\frac{\partial b_{w,i}}{\partial x}\hat{W}\right\rangle=0.$ 

Condition (C2) is similar to condition (C1), and is also imposed in [3] to simplify the verification of (21) and get a controller with a simple differential feedback form (see [10, III.A]). Condition (C3) states that each  $b_{w,i}$  forms a Killing vector for  $\hat{W}$ , which essentially ensures that the condition (21), evaluated using the perturbed dynamics (i.e., replacing  $\hat{A}$  in

(21) with A below (6)), does not depend on w. Now we are ready to build a connection between the CCM-based approach in [3] and our approach.

**Lemma 3.** Assume there exists a metric  $\hat{W}(x)$ , a matrix function  $\hat{Y}(x)$ , and a constant  $\hat{\lambda} > 0$  satisfying (21) and Assumption 2. Then, (13) and (14) with  $C = I_n$  and D = 0(corresponding to q(x, u) = x) can be satisfied with

$$W(x) = a\hat{W}(x), \ Y(x) = a\hat{Y}(x), \ \lambda = \hat{\lambda}, \ \alpha = \mu = \hat{\alpha}, \ (24)$$

where  $a \triangleq \sup_{x \in \mathcal{X}} \bar{\sigma}(B_w(x)) / \sqrt{\bar{\beta} \beta}$ , and  $\hat{\alpha}$  is defined in (23).

According to Lemma 3, if we can find matrices  $\hat{W}$  and  $\hat{Y}$ and constants  $\hat{\lambda}$  satisfying the inequality (21)that guarantees the contraction of the nominal closed-loop system and ensures an  $\mathcal{L}_{\infty}$ -gain bound  $\hat{\alpha}$  from disturbances to states, we can obtain the same  $\mathcal{L}_{\infty}$ -gain bound using our approach (Theorem 1) if we choose W(x) and Y(x) in (13) and (14) to be the scaled versions of W(x) and Y(x) in (21), i.e., enforcing the constraints in (24). However, if we relax such constraints in the optimization problem  $\mathcal{OPT}_{RCCM}$ , we are guaranteed to obtain a less conservative bound  $\alpha$ , i.e.,  $\alpha \leq \hat{\alpha}$ . This observation is summarized in the following theorem with the straightforward proof omitted.

**Theorem 2.** Assume there exists a metric  $\hat{W}(x)$ , a matrix function  $\hat{Y}(x)$ , and a constant  $\hat{\lambda} > 0$  satisfying (21) and Assumption 2. Then, we can always find W(x), Y(x),  $\lambda > 0$ ,  $\mu > 0$  and  $\alpha \leq \hat{\alpha}$  satisfying (13) and (14) with  $C = I_n$  and D=0, where  $\hat{\alpha}$  is defined in (23).

Remark 6. Theorem 2 indicates that our proposed RCCM approach is guaranteed to yield a tighter tube for the actual states than the CCM approach in [3], under Assumption 2.

# VI. SIMULATION RESULTS

In this section, we apply the proposed approach to a planar VTOL vehicle (illustrated in Fig. 1) and a 3D quadrotor and perform extensive comparisons with the CCM-based approach in [3]. All the subsequent computations and simulations were done in Matlab R2021a. Matlab codes are available at github. com/boranzhao/robust\_ccm\_tube. Animations to visualize the simulation results are included in the attached video, which is also available at youtu.be/mrN5iQo7NxE.

### A. Planar VTOL vehicle

The state vector is defined as  $x = [p_x, p_z, \phi, v_x, v_z, \dot{\phi}]^{\top}$ , where  $p_x$  and  $p_z$  are the position in x and z directions, respectively,  $v_x$  and  $v_z$  are the slip velocity (lateral) and the velocity along the thrust axis in the body frame of the vehicle,  $\phi$  is the angle between the x direction of the body frame and the x direction of the inertia frame. The input vector  $u = [u_1, u_2]$  contains the thrust force produced by each of the two propellers. The dynamics of the vehicle and details about the implementation can be found in the extended version of this paper [16].

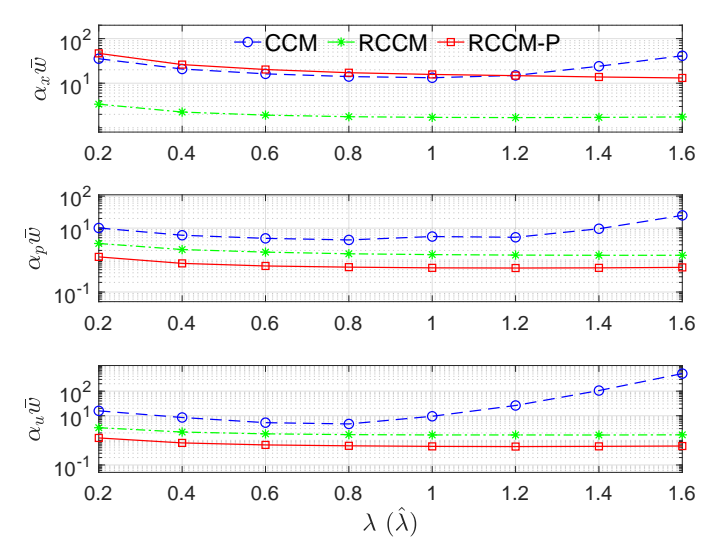


Fig. 2: Tube size for all states (top), position states (middle) and inputs (bottom) versus  $\lambda$  value under disturbances bounded by  $\bar{w}=1$ 

1) Computation of CCM/RCCM and associated tubes: We parameterize both the RCCM W and the CCM  $\hat{W}$  as polynomial matrices in  $(\phi, v_x)$  with up to degree 4 monomials. For a fair comparison of the proposed RCCM-based approach and the CCM-based approach in [3], we use same parameters when searching for CCM and RCCM whenever possible. We first consider the optimization of the tube size for all the states, as considered in [3]. For simplicity, we did not use weights for the states. For RCCM synthesis, we include a penalty for large control efforts when solving  $\mathcal{OPT}_{RCCM}$  by setting g(x, u) = $[x^{\top}, u^{\top}]^{\top}$ , and denote the resulting controller as **RCCM**. Additionally, we design another RCCM controller with a focus on optimizing the tubes for the position states and inputs, denoted as **RCCM-P**, by setting  $g(x, u) = [p_x, p_z, u^{\top}]^{\top}$ . We denote the controller designed using the CCM approach in [3] as CCM.

We consider a disturbance along the x direction of the inertia frame with effective acceleration up to 1 m/s (i.e., W = 1), which is 10 times as large as the disturbance considered in [3]. We swept through a range of values for  $\lambda$  (setting  $\hat{\lambda} = \lambda$ ) and solved the  $\mathcal{OPT}_{RCCM}$  in Section III-B to search for the RCCM and the optimization problem in [3, Section 4.2] to search for the CCM, using SOS techniques with YALMIP [17] and Mosek solver [18]. After obtaining the RCCM, we further solved  $\mathcal{OPT}_{REF}$  in Section III-C by gridding the state space to get refined tubes for different variables. The results are shown in Fig. 2. According to the top plot, while both controllers focused on optimizing the tube size for all states without using weights, RCCM yielded a much smaller tube than CCM. RCCM-P yielded a tube of similar size for all states compared to CCM, which came as no surprise since RCCM-P focused on minimizing the tube size for position states only, i.e.,  $(p_x, p_z)$ . From the middle and bottom plots, one can see that RCCM-P yielded much smaller tubes for both position states and inputs than RCCM, which further outperforms CCM by a large margin. For subsequent tests and simulations, we selected a best  $\lambda$  value for each of

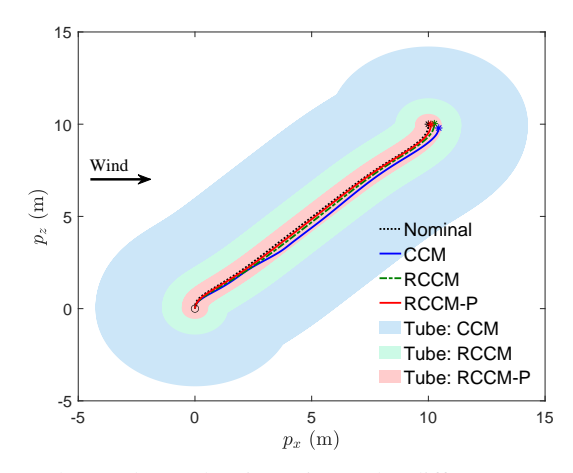


Fig. 3: Tubes and actual trajectories under different controllers the three controllers in terms of tube size for  $(p_x, p_z)$ , since the vehicle position is of more importance in tasks with collision-avoidance requirements. The best values for CCM, RCCM,

RCCM-P are determined to be 0.8, 1.4 and 1.2, respectively.

2) Trajectory tracking and verification of tubes: To test the trajectory tracking performance of the three controllers in scenarios and evaluate the conservatism with the derived tubes, we considered a task of navigation from the origin to target point (10, 10). We first planed a nominal trajectory with the objective of minimal force and minimal travel time, where the state constraint  $h(x) \geq 0$ , used in searching for CCM/RCCM, was enforced. With the nominal state and input trajectories, we simulated the performance of controllers in the presence of a wind disturbance, artificially simulated by  $w(t) = 0.8 + 0.2\sin(2\pi t/10)$ . The results of the position trajectories along with the tubes projected to the  $(p_x, p_z)$  plane are shown in Fig. 3. First, it is clear that the actual trajectory under each controller always stays in the associated tube. Second, in terms of tracking performance, RCCM-P and CCM perform the best and worst, respectively.

We further incorporated the three controllers in feedback motion planning for navigation in the presence of obstacles. Due to space limit, the results are included in [16].

# B. 3D quadrotor

The 3D quadrotor model is taken from [3] the state-space representation given has  $[p_x, p_y, p_z, \dot{p}_x, \dot{p}_y, \dot{p}_z, \tau, \phi, \theta, \psi]^{\top}$ , where the position  $p = [p_x, p_y, p_z]^{\top} \in \mathbb{R}^3$  and corresponding velocities are expressed in the global inertial (vertical axis pointing down) frame. Adopting the North-East-Down frame convention for the quadrotor body and the XYZ Euler-angle rotation sequence, the attitude (roll, pitch, yaw) is parameterized as  $(\phi, \theta, \psi)$  and  $\tau > 0$  is the total (normalized by mass) thrust generated by the four rotors. For controller design, we consider  $u \triangleq [\dot{\tau}, \dot{\phi}, \dot{\theta}]^{\top}$  as the control input. The actual implementation embeds the  $\dot{\tau}$  term within an integrator, and the resulting thrust and angular velocity reference (after being converted to body rate reference) are passed to a lower-level controller that is assumed to operate at a much faster time-scale. Given this parameterization, the dynamics of the quadrotor may be written as

$$\begin{bmatrix} \ddot{p}_x \\ \ddot{p}_y \\ \ddot{p}_z \end{bmatrix} = ge_3 - \tau \hat{b}_z + w = \begin{bmatrix} -\tau \sin(\theta) + w_2 \\ \tau \cos(\theta) \sin(\phi) + w_1 \\ g - \tau \cos(\theta) \cos(\phi) + w_3 \end{bmatrix}, (25)$$

where g is the local gravitational acceleration,  $e_3 = [0, 0, 1]^{\top}$ ,  $\hat{b}_z$  is the body-frame z-axis, and  $w = [w_1, w_2, w_3]^{\top} \in \mathbb{R}^3$  denotes the disturbance. We impose the following bounds:  $(\phi, \theta) \in [-60^{\circ}, 60^{\circ}]^2$ ,  $\tau \in [0.5, 2]g$ ,  $(\dot{\phi}, \dot{\theta}) \in [-180^{\circ}/s, 180^{\circ}/s]^2$ , and  $\dot{\tau} \in [-5, 5]g/s$ , which are sufficient for fairly aggressive maneuvers. Since yaw control is not a focus here, we simply set  $\dot{\psi} = 0$ .

1) Computation of CCM/RCCM and tubes: We parameterized both the RCCM W and the CCM W as polynomial matrices in  $(\tau, \phi, \theta)$  with up to degree 3 monomials. Additionally, the top left  $6 \times 6$  block of  $\hat{W}$  was imposed to be constant, i.e., independent of  $(\tau, \phi, \theta)$  to ensure that the resulting synthesis condition does not depend on u (see [3] for details). The RCCM synthesis condition (13), however, depends on  $(\dot{\tau}, \phi, \theta)$ , which is why we impose the bounds on  $(\dot{\tau}, \phi, \theta)$ mentioned above. Similar to Section VI-A, we first considered all states in optimizing the tube size. For simplicity, we did not use weights for the states. For RCCM synthesis, we included a penalty for large control efforts when solving  $\mathcal{OPT}_{RCCM}$  by setting  $g(x,u) = [x^{\top}, 0.02\dot{\tau}, 0.05\dot{\phi}, 0.05\dot{\theta}]^{\top}$ , and denote the resulting controller as RCCM. We designed another RCCM controller by optimizing the tubes for the position states only. For this, we set  $g(x, u) = [p_x, p_y, p_z, 0.02\dot{\tau}, 0.05\phi, 0.05\theta]^{\top}$ and denote the resulting controller as RCCM-P. We additionally designed a CCM controller and computed the associated tubes by following [3]. Through numerical experimentation, we found that imposing the lower bound constraint  $W \geq$  $0.01I_9$  yielded good performance for searching W, while imposing the constraint  $\hat{W} \geq I_9$  yielded good performance when searching  $\hat{W}$ . We swept through a range of values from 0.4 to 3.6 for  $\lambda$  (setting  $\hat{\lambda} = \lambda$ ) and solved the  $\mathcal{OPT}_{RCCM}$  in Section III-B to search for the RCCM and the optimization problem in [3, Section 4.2] to search for the CCM. We first tried the SOS technique used in Section VI-A to solve the involved optimization problems, but found it was not reliable especially for RCCM synthesis, taking notoriously long time while still yielding unsatisfactory results. Therefore, we eventually chose to grid the set of  $(\tau, \phi, \theta)$  (and additionally  $(\dot{\tau}, \dot{\phi}, \dot{\theta})$  for RCCM search), and solved the resulting optimization problem with a finite number of LMIs with YALMIP [17] and Mosek solver [18]. After obtaining the RCCM, we further solved  $\mathcal{OPT}_{REF}$  in Section III-C using the gridding technique to get refined tubes for different variables. The results in terms of tube size gain are shown in Fig. 4. As shown in the top plot, while both controllers focused on optimizing the tube size for all states without using weights, RCCM yielded a much smaller tube than CCM. RCCM-P yielded a tube of similar size for all states compared to CCM, which came as no surprise since RCCM-P focused on minimizing the tube size for position states only. From the bottom plot, one can see that RCCM-P yielded much smaller tubes for the position states than RCCM, which further outperformed CCM when  $\lambda$ 

is less than 2. Note that Assumption 2 does not hold anymore for this example, as the condition (C2) cannot be satisfied. Therefore, we cannot *guarantee* that RCCM will yield tighter tubes for all the states than CCM by applying Theorem 2.

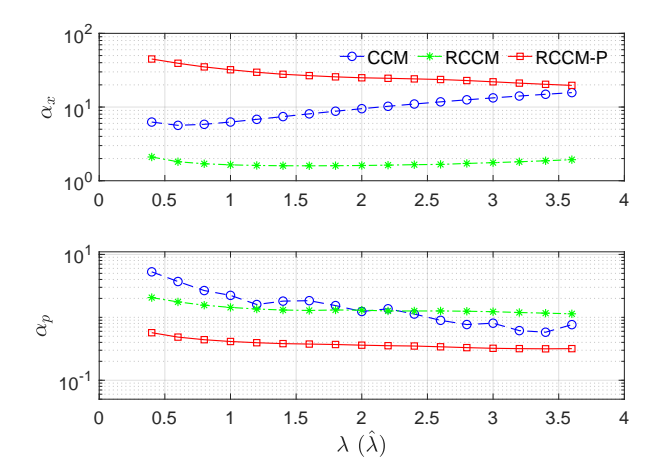
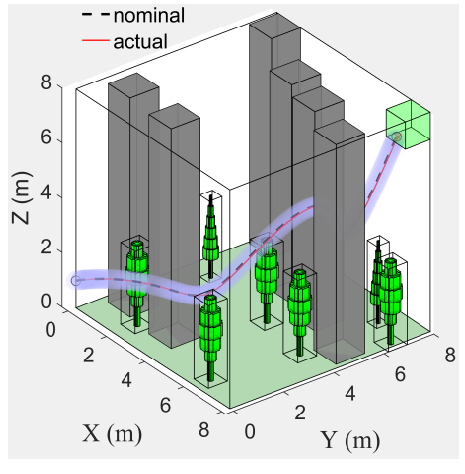
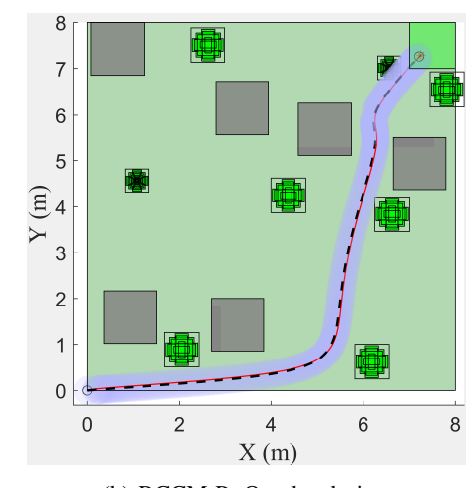


Fig. 4: Tube size gain for all states (top) and position states (bottom) versus  $\lambda$  ( $\hat{\lambda}$ ) value

2) Feedback motion planning and tracking in cluttered environments: To verify the controller performance, we randomly initialize the obstacle environments for the quadrotor, depicted in Fig. 5. The task for the quadrotor is to navigate from the start point  $[0,0,0]^{\top}$  to the goal region, depicted by the light green box, while avoding collisions. We considered a wind disturbance of up to 1 m/s², i.e.,  $||w|| \leq \bar{w} = 1$ . Due to space limit, we just show the performance of RCCM-P, which yielded a tube of a 0.32 m radius ball (i.e.,  $\alpha_p \bar{w} = 0.32$ ) for position coordinates at  $\lambda = 3.4$  under the aforementioned disturbance setting. The performance of CCM and the details of trajectory planning leveraging the tubes for position states are included in [16].

For simulation, RCCM-P was implemented using zeroorder-hold at 250 Hz. The Euler angular rates  $(\dot{\phi}, \dot{\theta})$ , computed by the CCM/RCCM-P, and  $\psi$  (which was set to constant zero) were converted to desired body rates, which were then sent to a low-level proportional controller. The P controller computed the three moments to track the desired body rates. The moments and the total thrust (from integrating  $\dot{\tau}$ ) were then applied as ultimate inputs to the quadrotor, which consists of 12 states. The planned and actual trajectories together with the projected tubes for position coordinates under RCCM-P and a wind disturbance, artificially simulated by w(t) = $(0.8 + 0.2\sin(0.2\pi t)) [\sin(45^\circ), -\cos(45^\circ), 0],$  are depicted in Fig. 5. One can see that the actual position trajectory was fairly close to the nominal one and consistently stayed in the ellipsoidal tubs. To evaluate the conservatism of the derived theoretical bounds associated with RCCM-P, we performed tests under incrementally increased disturbances. The results are shown in Fig. 6. According to Fig. 6, the tracking error under a disturbance bounded by  $\bar{w} = 6$  violated the theoretical bound associated with  $\bar{w}=1$  for the tested disturbance setting, indicating that the tube for position states was not very conservative. Trajectories of other states and control inputs are included in [16].





(a) RCCM-P: Isometric view

(b) RCCM-P: Overhead view

Fig. 5: Planned nominal and actual trajectories in an obstacle-rich environment under the RCCM-P. Actual trajectories consistently stay in the (light blue shaded) ellipsoidal tubes around the nominal trajectories.

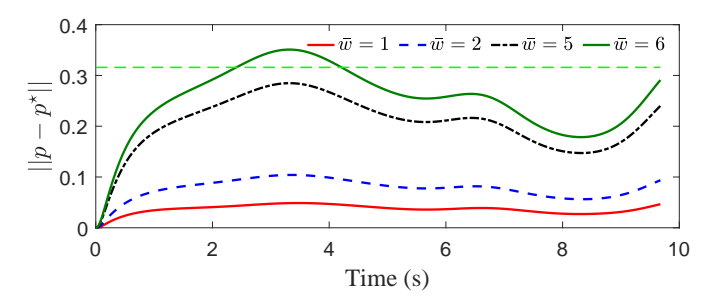


Fig. 6: Tracking error for the position states. The green dashed line denotes the theoretical bound associated with  $\bar{w} = 1$ .

#### VII. CONCLUSION

For nonlinear control-affine systems subject to bounded disturbances, this paper presents robust control contraction metrics (RCCM) for designing trajectory tracking controllers with explicit disturbance rejection properties and certificate tubes around any feasible nominal trajectories, for both states and inputs, in which the actual trajectories are guaranteed to remain despite disturbances. Both the RCCM controller and the tubes can be computed, offline, by solving convex optimization problems and conveniently incorporated into a feedback motion planning framework. Simulation results for a planar VTOL vehicle and a 3D quadrotor verify the effectiveness the proposed approach.

Future work includes testing of the proposed method on real hardware and leveraging the proposed method to deal with unmatched uncertainties within an adaptive control framework [12].

#### REFERENCES

- B. T. Lopez, J.-J. Slotine, and J. P. How, "Robust collision avoidance via sliding control," in *IEEE International Conference on Robotics and Automation (ICRA)*, pp. 2962–2969, 2018.
- [2] Z. Manchester and S. Kuindersma, "Robust direct trajectory optimization using approximate invariant funnels," *Autonomous Robots*, vol. 43, no. 2, pp. 375–387, 2019.
- [3] S. Singh, B. Landry, A. Majumdar, J.-J. Slotine, and M. Pavone, "Robust feedback motion planning via contraction theory," *The International Journal of Robotics Research*, submitted, 2019.

- [4] R. Tedrake, I. R. Manchester, M. Tobenkin, and J. W. Roberts, "LQR-trees: Feedback motion planning via sums-of-squares verification," *The International Journal of Robotics Research*, vol. 29, no. 8, pp. 1038–1052, 2010.
- [5] A. Majumdar and R. Tedrake, "Funnel libraries for real-time robust feed-back motion planning," *The International Journal of Robotics Research*, vol. 36, no. 8, pp. 947–982, 2017.
- [6] D. L. Marruedo, T. Alamo, and E. F. Camacho, "Input-to-state stable MPC for constrained discrete-time nonlinear systems with bounded additive uncertainties," in *Proc. CDC*, vol. 4, pp. 4619–4624, 2002.
- [7] B. T. Lopez, J.-J. E. Slotine, and J. P. How, "Dynamic tube MPC for nonlinear systems," in *Proc. ACC*, pp. 1655–1662, 2019.
- [8] J. Köhler, R. Soloperto, M. A. Müller, and F. Allgöwer, "A computationally efficient robust model predictive control framework for uncertain nonlinear systems," *IEEE Transactions on Automatic Control*, vol. 66, no. 2, pp. 794–801, 2020.
- [9] W. Lohmiller and J.-J. E. Slotine, "On contraction analysis for non-linear systems," *Automatica*, vol. 34, no. 6, pp. 683–696, 1998.
- [10] I. R. Manchester and J.-J. E. Slotine, "Control contraction metrics: Convex and intrinsic criteria for nonlinear feedback design," *IEEE Transactions on Automatic Control*, vol. 62, no. 6, pp. 3046–3053, 2017.
- [11] H. Tsukamoto and S.-J. Chung, "Robust controller design for stochastic nonlinear systems via convex optimization," *IEEE Transactions on Automatic Control*, vol. 66, no. 10, pp. 4731–4746, 2020.
- [12] A. Lakshmanan, A. Gahlawat, and N. Hovakimyan, "Safe feedback motion planning: A contraction theory and L<sub>1</sub>-adaptive control based approach," in *Proceedings of 59th IEEE Conference on Decision and Control (CDC)*, pp. 1578–1583, 2020.
- [13] P. Zhao, Z. Guo, Y. Cheng, A. Gahlawat, and N. Hovakimyan, "Guaranteed contraction control in the presence of imperfectly learned dynamics," *Annual Conference on Learning for Dynamics and Control*, under review, 2022. arXiv:2112.08222.
- [14] I. R. Manchester and J.-J. E. Slotine, "Robust control contraction metrics: A convex approach to nonlinear state-feedback  $H_{\infty}$  control," *IEEE Control Systems Letters*, vol. 2, no. 3, pp. 333–338, 2018.
- [15] C. Scherer, P. Gahinet, and M. Chilali, "Multiobjective output-feedback control via LMI optimization," *IEEE Transactions on Automatic Control*, vol. 42, no. 7, pp. 896–911, 1997.
- [16] P. Zhao, A. Lakshmanan, K. Ackerman, A. Gahlawat, M. Pavone, and N. Hovakimyan, "Tube-certified trajectory tracking for nonlinear systems with robust control contraction metrics," arXiv preprint arXiv:2109.04453, 2021.
- [17] J. Lofberg, "YALMIP: A toolbox for modeling and optimization in MATLAB," in *Proceedings of 2004 IEEE International Symposium on Computer Aided Control Systems Design*, pp. 284–289, 2004.
- [18] E. D. Andersen and K. D. Andersen, "The MOSEK interior point optimizer for linear programming: An implementation of the homogeneous algorithm," in *High Performance Optimization*, pp. 197–232, Springer, 2000.